

# ANALYSIS OF INDUCTION MOTOR PERFORMANCE IN ELECTRIC VEHICLES USING NUMERICAL SIMULATION

Shoaib Khan<sup>1</sup>, Sooraj Kumar Chourasia<sup>2</sup>, Bablu Patel<sup>3</sup> and Sakshi Soni<sup>4</sup>

Department of Electrical and Electronics Engineering, Eklavya University, Damoh, M.P.

[shoaibkhannoori@gmail.com](mailto:shoaibkhannoori@gmail.com)

[sooraj0894@gmail.com](mailto:sooraj0894@gmail.com)

[patelbablu94@gmail.com](mailto:patelbablu94@gmail.com)

[sonisakshi640@gmail.com](mailto:sonisakshi640@gmail.com)

**Abstract**—Electric vehicles (EVs) are becoming more popular than traditional vehicles powered by fossil fuels. However, the higher cost of an EV's purchase means that it may remain a major roadblock for the market. Customers choose electric vehicles for a variety of reasons, including lower carbon emissions, better performance, and more. Environmental awareness and a vision for renewable energy are essential to ensuring the long-term viability of energy production. According to a recent study, the demand for electric vehicles will rise by 2-6 percent for every 1 percent increase in renewable energy sources. By altering the recharging power at a given time interval, electric vehicles (EVs) can offer new potential for delivering regulation services and a wide range of consumption options. Modeling electric vehicles is the primary subject of this paper. A Rinehart motion systems-AC motor controller- 'PM100DZ' will be used to replicate the performance of an Evo-electric 'AF-130' Permanent Magnet Synchronous Motor. Using this data, researchers are able to better understand how permanent-magnet motor drives work. Simscape blocks used to model PMSM and vector control are to be validated in this effort. As a last step, parameter estimation is used to tweak the Dynamic motor and Thermal models. Datasheet values and simulated data still differed, and this difference is investigated to determine its source.

**Keywords**—Photovoltaic (PV), Electrical Vehicle, Characteristic Analysis, Design Simulation, Modeling

## I. INTRODUCTION

Electric vehicles (EVs) are gaining popularity around the world, outpacing traditional fossil-fuel vehicles. However, because batteries are far more expensive, the purchase price of an EV may remain the primary market barrier. Customers choose EVs for a variety of

reasons, including less environmental impact due to zero carbon emissions, increased performance, and so on. Consumers that are environmentally conscious and have a vision for renewable energy are necessary for energy sustainability. According to recent research, a 1% increase in renewable energy would result in an approximately 2–6% rise in EV demand. The issues of electric vehicle (EV) charging stations are examined in this chapter, as well as the expanding use of distributed generators in today's electrical grid. The advantages of using photovoltaic (PV) sources in conjunction with battery storage systems are discussed. Finally, the chapter concludes with an overview of the proposed system's high-level design as well as a synopsis of the information in the next chapters.

The impending scarcity of fossil fuels and the current environmental constraints of lowering greenhouse gas emissions have prompted substantial research into electric vehicles (EVs) [1-3]. Consumer desire to move from traditional internal combustion engine vehicles to EVs as an alternative mode of transportation, however, has a significant impact on EV development. This willingness is the most important component in predicting future EV demand. The authors concluded that one of the major issues facing the EV market is charging time. [4-6] As a result, the focus of this paper is on developing unique ways for minimizing EV charging time by implementing rapid charging rates. In the United States, three levels of EV charging (illustrated in Fig. 1.1) are being researched and developed. The charging levels of electric vehicles are classed based on their power charging rates [7-9].

Overnight charging occurs in level I, with the EVs plugged into a handy power outlet (120 V) for sluggish

charging (1.5-2.5 kW) over long periods of time. The main disadvantage of level-I charging is the long charging time, which makes it unsuitable for long driving cycles requiring many charging operations. Furthermore, from the perspective of electrical grid operation, the long charging hours at night overburden distribution transformers, which are not allowed to rest in a grid system with a large number of linked EVs [10]. Level-II charging necessitates a 240 V outlet; as a result, it is frequently utilised as the principal charging method in both private and public facilities. This charging level can restore exhausted EV batteries by giving power in the range of 4 - 6.6 kW over a 3 - 6 hour period [11]. The biggest disadvantage of this charging level is the time required. Furthermore, voltage sags and substantial power losses in an electrical grid system with a large penetration of level II charging are two of the obstacles that the widespread use of the technology faces. Control and coordination at level II would mitigate the detrimental effects of level-II charge [12], but this would necessitate the implementation of a comprehensive communication system.

Three types of chargers for EV charging stations are shown in Figure 1.

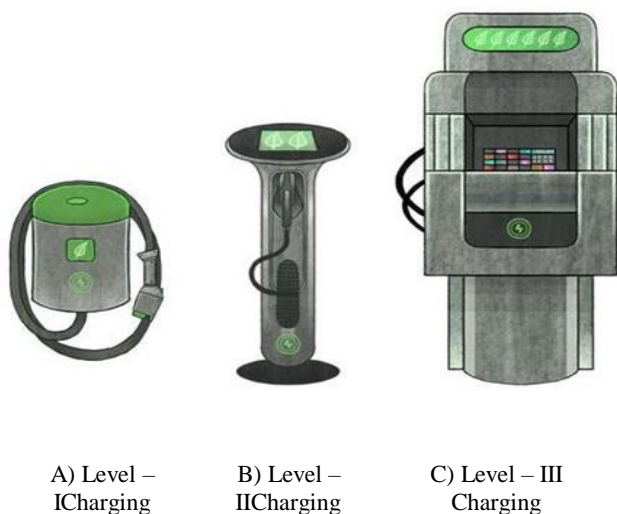


Fig. 1 Three levels of chargers for EV charging stations [13]

## II. PROPOSED METHODOLOGY

The Double Cage Induction motor is that type of motor in which a double cage or two rotor windings or cages are used. This arrangement is used for obtaining high starting torque at a low value of starting current. The motor controller converts the DC power from the vehicle Energy Storage System to the 3-phase AC

required by the motor. The PM100DZ uses the Vector control technology for controlling the torque output of the motor.

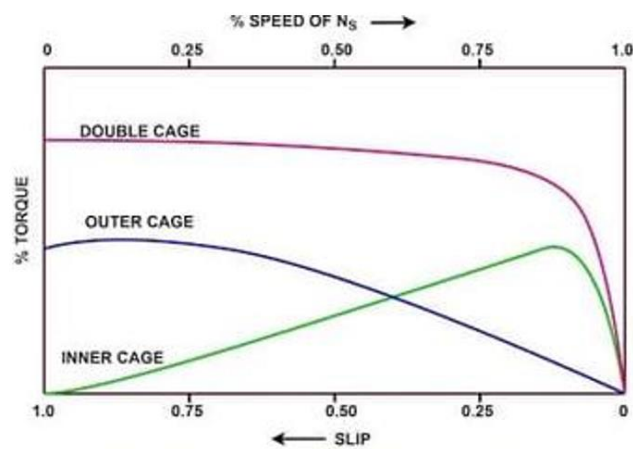


Fig. 2 Torque-Speed Characteristics of Double Cage Induction Motor

TABLE I

Description of Protection Scheme- Vehicle

Parameters	Specifications
Short Circuit Protection	Yes
Hardware Over-current Protection	Yes
Vehicle System Power	9.. 16VDC (12V Systems)
Operating Temperature Range – coolant water – no derating	-40 +80°C
Isolation – High-Voltage to Low-Voltage	1000Vrms
Isolation – High-Voltage to Case	1000Vrms
Isolation – Low-Voltage to Case	50V
Operating Temperature Range – coolant water – derated output power	-40.. +105°C
Non-Operating Temperature	-40 .. +115°C
Storage Temperature	-55 .. +105°C
Coolant Type	50/50 EGW
Coolant Flow Rate	8 – 12 LPM
Coolant Pressure Drop	0.2 bar for PM100xx
Maximum Coolant Pressure (above ambient)	1.4 bar
Operating Shock (ISO 16750-3, Test 4.2.2.2)	500 m/s <sup>2</sup> (50g)

Operating Vibration (ISO 16750-3, 4.1.2.4 Test IV)	27.8 m/s <sup>2</sup> (3grms)
Environmental Protection Class	IP6K9K

TABLE II

Specifications of Motor Used in Proposed Simulation

Parameters	Specifications
Type	Asynchronous- Double Squirrel Cage
Maximum Speed	8000 rpm
Nominal Torque	145 Nm
Peak Torque (for up to 60s)	250Nm
Peak Torque (for up to 20s)	350Nm
Nominal Output Power	121.47 kW
Peak Output Power (for up to 60s)	209.43 kW
Peak Output Power (for up to 20s)	293.21 kW
Torque Density	11.5Nm/kg
Power Density	4.6kW/kg
Peak Efficiency	95.10%
Coolant Medium	Water/Glycol (50/50)
Coolant Flow Rate	> 8l/min
Dimensions	110 mm (L) x 300 mm (D)at 30.5 kg

### III MATHEMATICAL MODELING OF DOUBLE SQUIRREL CAGE INDUCTION MOTOR (DSCIM)

The DSCIM and SM both have similar stator and wound rotor respectively, the induced currents in the rotor of DSCIM are negligible and both produce similar back EMF. Hence the mathematical model of a DSCIM is similar to that of the wound rotor. Therefore, the d-q equations of the PMSM are:

$$v_q = Ri_q + p\lambda_q + \omega_s\lambda_d \quad (1)$$

$$v_d = Ri_d + p\lambda_d + \omega_s\lambda_q \quad (2)$$

Where,

$$\lambda_q = L_q i_q; \quad \lambda_d = L_d i_d + \lambda_{af}$$

$v_d$  and  $v_q$  are q and d axis voltage,  $i_q$  and  $i_d$  are q and d axis stator current,  $i_d$  and  $i_q$  are the d, q axis stator currents,  $L_d$  and  $L_q$ , are the d, q axis inductances,  $\lambda_d$  and  $\lambda_q$ , are the d, q axis stator flux linkages, while  $R$  and  $\omega_s$ , are the stator resistance and inverter frequency, respectively.  $\lambda_{af}$  is the flux linkage due to the rotor magnets linking the stator. The electric torque is

$$T_e = \frac{3P[\lambda_{af}i_q + (L_d - L_q)i_d i_q]}{2} \quad (3)$$

And the equation of motor dynamics is

$$T_e = T_L + B\omega_r + Jp\omega_r \quad (4)$$

$P$  is the number of pole pairs,  $T_L$  is the load torque,  $B$  is the damping coefficient,  $\omega_r$ , is the rotor speed, and  $J$  is the moment of inertia. Simscape comes with a general model of the DSCIM machines here are a few details about the Simscape Asynchronous Machine block:

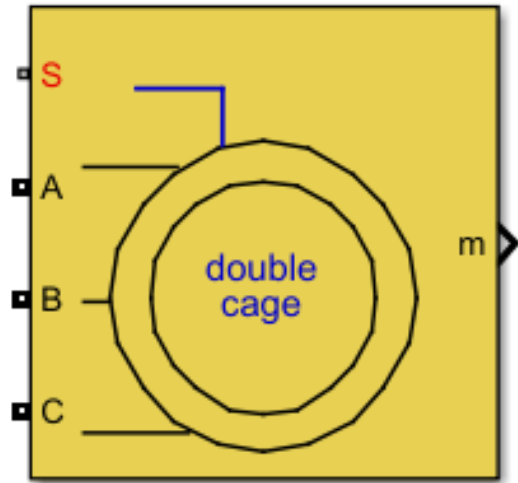


Fig. 3 Simulink Block of Double Squirrel Cage Induction Motor

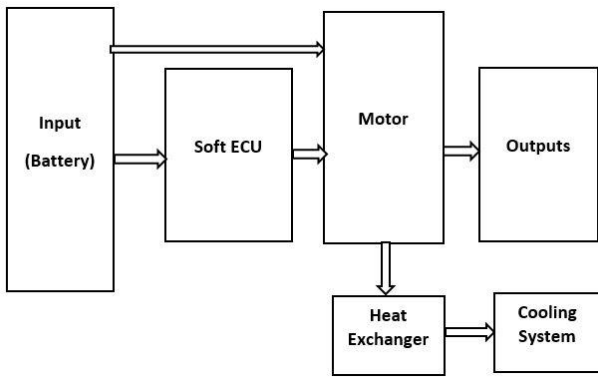


Fig. 4 Block Diagram of Controlled Vehicle System

The Double Squirrel Cage Induction Machine block operates in either generator or motor mode. The mode of operation is dictated by the sign of the mechanical torque (positive for motor mode, negative for generator mode). The heat generated is determined by the difference between the electric power from Battery and the mechanical power generated hence this heat accounts for heat generated in MCU and motor both.

#### IV. SIMULATION ANSD RESULTS

##### MODELLING OF SYSTEM USING SIMSCAPE BLOCK

TABLE III

Important Simulation Parameters

Parameters	Value	Parameters	Value
Ts	1.00E-05	Resistance	0.11607
Stator phase resistance	0.0490392	Flux by magnet	0.17491
Armature inductance	6.32E-04	Temp_amb	300
Flux linkage	0.17216	Coolant_cp	400.07
Pole pairs	3	Coolant_mass	2.2147
Induced flux	0.17197	hac	30.3749
Current hysteresis band	0.1	hcm	35.286
Snubber resistance	1.00E+04	Area_ht	3
Ron	7.83E-06	motor_cp	12.5
Inrt	2.50E-04	radiator_area	2.3951

Damp	4.18E-04	motor_mass	30
battery Voltage	390.4254		

The parameter estimation is done separately for motor dynamics and thermal to improve performance. Due to low Simulation speed, it is very difficult to simulate the test for whole 1288 secs therefore, for testing and simulation a 200 sec of data clip has been taken from the test data and then the result is obtained.

Since many variables for modelling the motor are unknown, we will create single value variables for those parameters so that we can utilize them for parameters estimation. A step-by-step modelling guide is not needed as most of the blocks are present in Simscape understanding the functionality and parameter estimation is given focus.

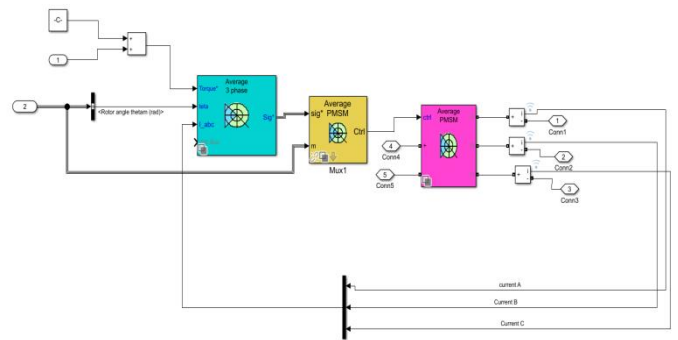


Fig. 5 Implementation of Proposed Vector Control Methodology

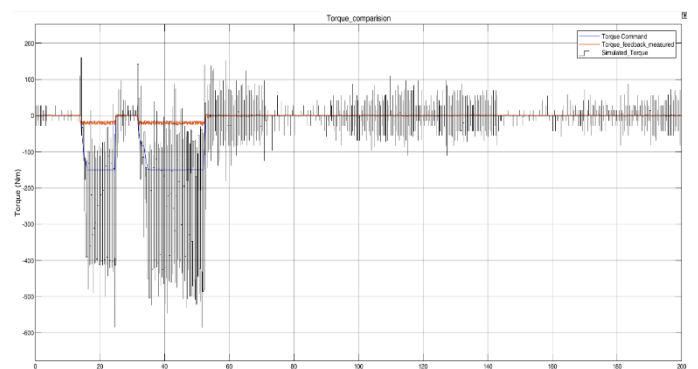


Fig. 6 Torque Analysis of Proposed System

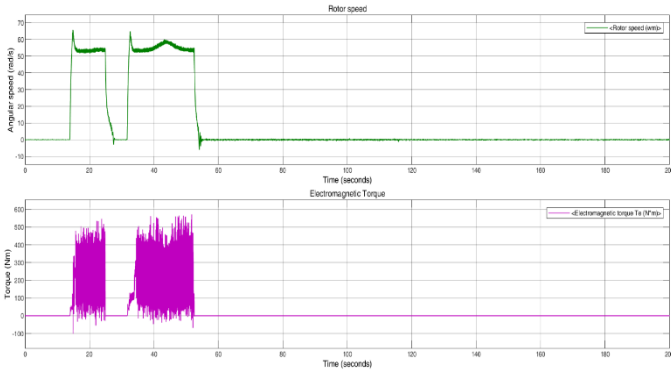


Fig. 7 Rotor Speed and Electromagnetic Torque

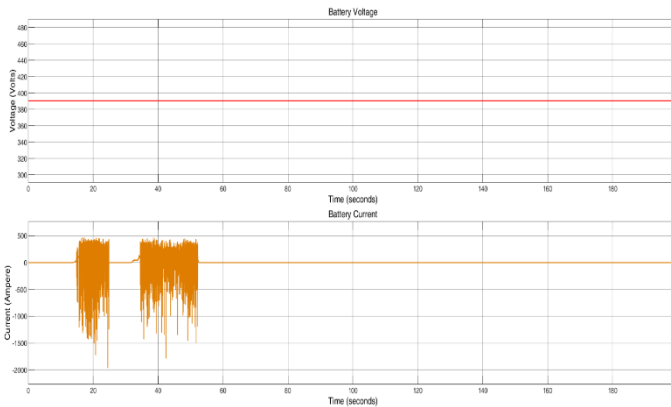


Fig. 8 Battery Voltage and current

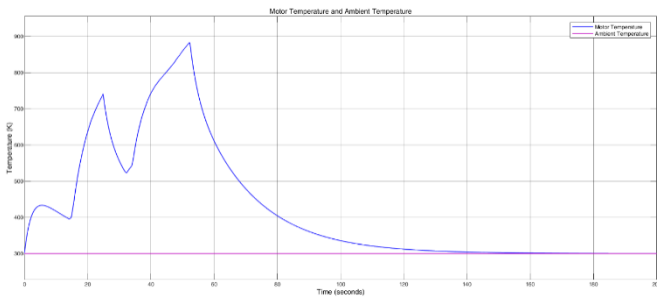


Fig. 9 Temperature Analysis

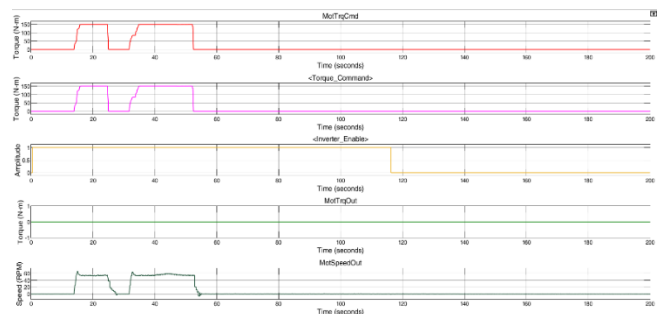


Fig. 10 Soft MCU Outputs

When the initial torque command is fired, the motor is unable to meet the torque demand and just provides 20% of the torque demand. There are two possibilities for

this. One, a mistake in setup but it seems unlikely as the later torque demand is successfully met, another possible reason for this could be that the damper windings are used to run the machine up to speed on induction motor action with the machine pulling into synchronism by a combination of the reluctance and synchronous motor torques provided by the magnet. During the startup, the magnet exerts a braking torque that opposes the induction-motor-type torque provided by the damper windings.

## V.CONCLUSION

The Double Squirrel Cage Induction Motor is modelled for different speeds and the phase currents. By implementing the Average Field oriented control method, the phase currents are converted into the desired data type. The motor is unable to match the torque demand when the initial torque instruction is issued, and only offers 20% of the torque need. This could be one of two things. One possibility is that the damper windings are used to run the machine up to speed on induction motor action, with the machine pulling into synchronism by a combination of the reluctance and synchronous motor torques provided by the magnet. Another possibility is that "Damper windings are used to run the machine up to speed on induction motor action, with the machine pulling into synchronism by a combination of the reluctance and synchronous motor torques provided by the magnet during start-up, the magnet produces a braking torque that resists the damper windings' induction-motor-type torque. The second anomaly in the datasheet is the temperature measurement at the motor, value remains at 273K for few milli- seconds and then motor temperature increases and reaches up to 880.48K.

The first 0 results could be attributable to the sensor's reaction time, implying that the system is always at 300K. The passage of heat is initiated by the temperature difference between the two bodies. The motor remained at 300K throughout the trial, indicating that the coolant flow rate and torque requirement are perfectly synchronized, and hence all heat created is instantly absorbed by the coolant. Although we have devised a cooling mechanism that keeps the motor within a safe operating temperature range, this model can be adjusted to reflect genuine data when available, which seems exceedingly unlikely. Otherwise, the model is quite close to the motor's actual performance and is ready to be employed in systems that are more complicated.

## VI. REFERENCES

- [1] Badea, Gheorghe, Raluca-Andreea Felseghi, Mihai Varlam, Constantin Filote, Mihai Culcer, Mariana Iliescu, and Maria Simona Răboacă. "Design and simulation of romanian solar energy charging station for electric vehicles." *Energies* 12, no. 1, 2019.
- [2] Badea, Gheorghe, Raluca-Andreea Felseghi, Mihai Varlam, Constantin Filote, Mihai Culcer, Mariana Iliescu, and Maria Simona Răboacă. "Design and simulation of romanian solar energy charging station for electric vehicles." *Energies* 12, no. 1, 2019.
- [3] Mouli, G.C., Bauer, P. and Zeman, M., "System design for a solar powered electric vehicle charging station for workplaces", *Applied Energy*, 168, pp.434-443, 2016.
- [4] Vignesh, T. R., M. Swathisriranjani, R. Sundar, S. Saravanan, and T. Thenmozhi. "Controller for Charging Electric Vehicles Using Solar Energy." *Journal of Engineering Research and Application* 10, no. 01, pp. 49-53, 2020.
- [5] Suganthi, D., and K. Jamuna. "Charging and Discharging Characterization of Community Electric Vehicle Batteries." In *Emerging Solutions for e-Mobility and Smart Grids*, pp. 213-223. Springer, Singapore, 2021.
- [6] Harika, S., R. Seyezhai, and A. Jawahar. "Investigation of DC Fast Charging Topologies for Electric Vehicle Charging Station (EVCS)." In *TENCON 2019-2019 IEEE Region 10 Conference (TENCON)*, pp. 1148-1153. IEEE, 2019.
- [7] Gautham Ram Chandra Mouli, Pavol Bauer and Miro Zeman, "System design for a solar powered electric vehicle charging station for workplaces." *Applied Energy*, 2016.
- [8] Ravikant, U. Chauhan, V. Singh, A. Rani and S. Bade, "PV Fed Sliding Mode controlled SEPIC converter with Single Phase Inverter," 2020 5th International Conference on Communication and Electronics Systems (ICCES), pp. 20-25, 2020.
- [9] Xu, Tong, Hengshu Zhu, Xiangyu Zhao, Qi Liu, Hao Zhong, Enhong Chen, and Hui Xiong. "Taxi driving behavior analysis in latent vehicle-to-vehicle networks: A social influence perspective." In *Proceedings of the 22nd ACM SIGKDD International Conference on Knowledge Discovery and Data Mining*, pp. 1285-1294. 2016.
- [10] Saadullah, Aqueel Ahmad, Furkan Ahmad, Mahdi Shafaati Shemami, Mohammad Saad Alam, and Siddiq Khateeb, "A comprehensive review on solar powered electric vehicle charging system." *Smart Science* 6, no. 1, pp. 54-79, 2018.
- [11] Anderson, John Augustus. "Power-conditioned solar charger for directly coupling to portable electronic devices." U.S. Patent No. 9, 088,169. 21 Jul. 2015.
- [12] Guo, Qijie, et al. "Fabrication of 7.2% efficient CZTSSe solar cells using CZTS nanocrystals." *Journal of the American Chemical Society* 132.49, pp. 17384-17386, 2010.
- [13] A. Testa, S. De Caro, T. Scimone and S. Panarello, "A buck-boost based DC/AC converter for residential PV applications," *International Symposium on Power Electronics Power Electronics, Electrical Drives, Automation and Motion*, pp. 114-119, 2012.
- [14] Le, Hoai Nam, and Jun-Ichi Itoh. "Inductance-independent nonlinearity compensation for single-phase grid-tied inverter operating in both continuous and discontinuous current mode." *IEEE Transactions on Power Electronics*, 4904-4919, 2018.
- [15] Dahal, R., J. Li, K. Aryal, J. Y. Lin, and H. X. Jiang. "InGaN/GaN multiple quantum well concentrator solar cells." *Applied Physics Letters* 97, no. 7, 2010.
- [16] Kukde, Harsha, and A. S. Lilhare. "Solar powered brushless DC motor drive for water pumping system." 2017 International Conference on Power and Embedded Drive Control (ICPEDC). IEEE, 2017.
- [17] Nie, Wanyi, Hsinhan Tsai, Reza Asadpour, Jean-Christophe Blancon, Amanda J. Neukirch, Gautam Gupta, Jared J. Crochet and Millimeter Lawan, "High-efficiency solution-processed perovskite solar cells with millimeter-scale grains." *Science* 347, no. 6221, pp. 522-525, 2015.

- [18] Sahoo, Saroja Kanti, and Nudurupati Krishna Kishore. "Battery state-of-charge-based control and frequency regulation in the MMG system using fuzzy logic." *IET Generation, Transmission & Distribution*, 2020.
- [19] Ichikawa, Yukimi, Yoshiaki Osawa, Hiroshi Noge, and Makoto Konagai. "Theoretical studies of silicon hetero-junction solar cells with rib structure." *AIP Advances* 9, no. 6, 2019.
- [20] HariPriya, T., Alivelu M. Parimi, and U. M. Rao. "Performance evaluation of DC grid connected solar PV system for hybrid control of DC-DC boost converter." In 2016 10th IEEE International Conference on Intelligent Systems and Control (ISCO), pp. 1-6, 2016.
- [21] Simiran Kuwera, Sunil Agarwal and Rajkumar Kaushik, "Application of Optimization Techniques for Optimal Capacitor Placement and Sizing in Distribution System: A Review", *International Journal of Engineering Trends and Applications (IJETA)*, vol. 8, no. 5, Sep-Oct 2021.
- [22] T. Manglani, A. Vaishnav, A. S. Solanki and R. Kaushik, "Smart Agriculture Monitoring System Using Internet of Things (IoT)," *2022 International Conference on Electronics and Renewable Systems (ICEARS)*, Tuticorin, India, 2022, pp. 501-505.
- [23] T. Manglani, R. Rani, R. Kaushik and P. K. Singh, "Recent Trends and Challenges of Driverless Vehicles in Real World Application", *2022 International Conference on Sustainable Computing and Data Communication Systems (ICSCDS)*, pp. 803-806, 2022.
- [24] Saha, Swarup Kumar. "Optimization Technique Based Fuzzy Logic Controller for MPPT of Solar PV System." 2018 International Conference on Emerging Trends and Innovations In Engineering And Technological Research (ICETIETR). IEEE, 2018.
- [25] Patel, Hiren, and Vivek Agarwal. "MATLAB-based modeling to study the effects of partial shading on PV array characteristics." *IEEE transactions on energy conversion* 23.1, pp. 302-310, 2008.
- [26] Satapathy, Susree Sukanya, and Nishant Kumar. "Modulated Perturb and Observe Maximum Power Point Tracking Algorithm for Solar PV Energy Conversion System." 2019 3rd International Conference on Recent Developments in Control, Automation & Power Engineering (RDCAPE). IEEE, 2019.